

$I = \frac{3}{2}$ πN Resonances in the 1900-MeV Region*

R. E. Cutkosky and R. E. Hendrick
Carnegie-Mellon University, Pittsburgh, Pennsylvania 15213

and

R. L. Kelly
Lawrence Berkeley Laboratory, Berkeley, California 94720
(Received 7 June 1976)

We report results of a πN partial-wave analysis for $I = \frac{3}{2}$ resonances observed in the 1900-MeV region: $F_{35}(1885)$, $F_{37}(1945)$, $P_{31}(1940)$, and $D_{35}(1925)$. The $D_{35}(1925)$ is difficult to accommodate in conventional baryon models; we discuss an alternative model having such a state.

The $SU(6) \times O(3)$ harmonic-oscillator model proposed by Greenberg,¹ its relativistic² and diquark³ variations, and recent "dual string"⁴ and "bag"⁵ models have had notable success in reproducing the observed baryon mass spectrum. Primary information to test such models comes from partial-wave analyses. We report here initial results of a πN partial-wave analysis between 1550 and 2150 MeV. We concentrate on resonances observed in the F_{35} , F_{37} , P_{31} , and D_{35} partial waves around 1900 MeV. The even-parity states at this mass are placed by harmonic-oscillator quark models in a $(\underline{56}, 2^+)$ $SU(6) \times O(3)$ supermultiplet.⁶ However, the odd-parity $D_{35}(1925)$ is not readily accommodated by such models. We have performed additional tests which support the existence of the $D_{35}(1925)$, and present a model which provides a D_{35} resonance at this energy.

World πp elastic and charge-exchange scattering data were amalgamated at 26 momenta in the range $0.8 \leq p_{lab} \leq 2.0$ GeV/c. The amalgamated data were partial-wave analyzed by a combination of the accelerated convergence expansion (ACE) technique for an energy-independent fitting and a hyperbolic dispersion technique for the resolution of ambiguities and the imposition of s-channel analyticity constraints. The amalgamation took into account normalization errors, momentum calibration errors, discrepancies between experiments, correlated interpolation errors, and other systematic effects.⁷ Single-energy fits to these data were made using a parametrization with each invariant amplitude represented as a sum of a fixed "Born term" and a fitted polynomial term constructed according to the ACE prescription.⁸ The Born term contains contributions from Pomeron and peripheral di-pion exchange,⁹ and also from Reggeized ρ , f , N , and Δ exchange. The parametrization¹⁰ is analytic in the cut $\cos \theta$ plane,

with asymptotic power behavior $(\cos \theta)^{\alpha(s)}$ for large $|\cos \theta|$, and has no sharp cutoff in angular momentum. At each momentum, depending on the completeness of data, there were three to fifteen clusters of statistically indistinguishable local χ^2 minima. The covariance matrix estimated for each cluster includes the spread within the cluster.

To resolve ambiguities the reconstructed invariant amplitudes along four hyperbolic curves in the physical region of the s - t plane (supplemented by results of Carter *et al.*¹¹ and Ayed and Bayre¹² outside our energy range) were fitted with a parametrization based on hyperbolic dispersion relations (HDR).¹³ The HDR fit selected a unique cluster at each energy. To check and further stabilize these results, the input amplitudes at each energy in turn were deleted and HDR predictions were generated. These predictions, with enlarged errors, were then combined with the scattering data for a second round of energy-independent fitting. Results are shown in Fig. 1.

Resonances were parametrized using a smoothly varying background term and a modified Breit-Wigner resonance term for the partial-wave amplitudes: $T = T_B + S_B T_R$. The resonance amplitude is $T_R = a_1 \varphi_{el} / D_R$, with

$$D_R = s_0 - s - i a_1 \varphi_{el} - i \sum_k a_k a_{k+1} \varphi_k,$$

where s is the square of the center-of-mass energy, $\varphi_{el}(s)$ is an elastic phase-space factor, and $\varphi_k(s)$ are inelastic phase-space factors for the $\pi\pi N$ and quasi-two body channels such as $\pi\Delta$, ρN , ηN , ωN , and $\rho\Delta$. The coefficients a_i and s_0 are free parameters. The background amplitude is $T_B + (S_B - 1)2i$, where $S_B = D_- / D_+$ with

$$D_{\pm} = [1 + b_2 y \mp i \varphi_{el}(b_1 + y b_3)] \\ \times \{1 \pm \varphi_{el} \sum_k \varphi_k [(1-y)b_{2k+2}^2 + y b_{2k+3}^2]\}$$

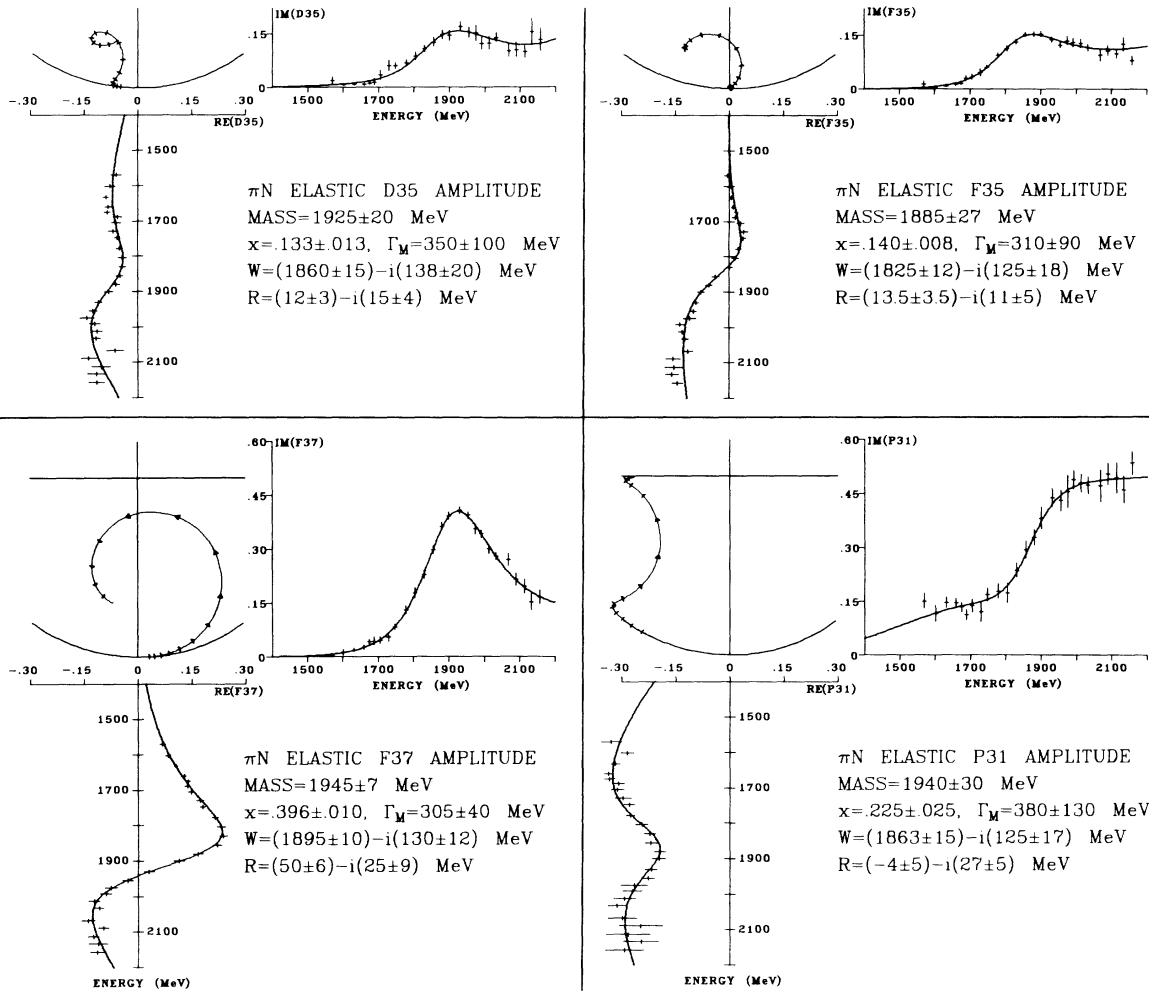


FIG. 1. $I = \frac{3}{2}$ πN resonances in the 1900-MeV region. Results of energy-independent fitting are shown as data points; energy-dependent partial-wave fits are shown as curves. The fit is also shown on the Argand plot, with arrows at multiples of 50 MeV.

and $y = [(s - \alpha)^{1/2} - (s_1 - \alpha)]^{1/2} / [(s - \alpha)^{1/2} + (s_1 - \alpha)^{1/2}]$. The coefficients b_i are free parameters, $s_1 = (M + 2\mu_\pi)^2$ is the three-body threshold, and α is a fixed parameter determining the onset of the cut in the left-hand s plane. The mass, width, elasticity, pole position, and residue were determined from a series of best fits. Errors on these parameters were estimated by a Monte Carlo procedure of varying the partial-wave data with correlated Gaussian distributions and by separately varying the form of the parametrization. The resonance mass is defined here to be the real center-of-mass energy at which the real part of D_R vanishes. The width Γ_M is defined by representing D_R as locally proportional to $E - M - i\Gamma_M/2$ at $E = M$; the elasticity is defined as $\alpha = [-\text{Im}(T_R^{-1})]^{-1}$. The pole position W is the com-

plex energy at which D_R vanishes, and the residue R of the pole includes the factor S_B .

Two systematic features of the resonances shown in Fig. 1 are the sizable difference between the real part of the pole position and the resonance mass, and the negative phase of the residues. These effects can be largely accounted for by the energy dependence of the width, although the backgrounds also contribute negative phases, especially for P_{31} . Another regular feature is the imaginary pole position being less than $\Gamma_M/2$, partly a result of the local definition of Γ_M . The pole position is generally more stable than M or Γ_M ,¹⁴ and its imaginary part is closer to the visual half-width than is $\Gamma_M/2$.

Three well established even-parity resonances were observed: $F_{35}(1885)$, $F_{37}(1945)$, and

$P_{31}(1940)$, all conventionally assigned to a $(\underline{56}, 2^+)$ supermultiplet. A significant result of our analysis is the confirmation of a D_{35} resonance at 1925 MeV. Other analyses¹⁵ have also reported a D_{35} resonance near 1900 MeV. Because the $D_{35}(1925)$ is not consistent with conventional $SU(6) \times O(3)$ models (see below) we have performed tests to insure that it is really required by the πN scattering data. New randomly started single-energy fits were made to the amalgamated scattering data at three energies in the resonance region, with the D_{35} constrained to a smooth background value and the HDR constraints omitted. At 1804 and 1900 MeV the amplitudes are particularly well determined because charge-exchange cross section and polarization data exist. At 1900 MeV the best χ^2 for a fit to the 226 data points was 210, to be compared with 176 obtained for the best fit using HDR constraints, and the χ^2 for 103 π^+p data points increased from 75 to 102. At 1804 and 1856 MeV somewhat larger increases in χ^2 were found. In fits with the D_{35} resonance removed, there was a tendency for the G_{39} partial wave to develop anomalous ancestorlike behavior. These direct tests confirmed studies based on the partial-wave covariance matrix, which showed that the resonant behavior of the D_{35} was associated with observable quantities rather than with unobservable phases.

A detailed report of other partial-wave fits will be published later, but we mention here results relevant to the $SU(6) \times O(3)$ classification. We see all πN resonances conventionally assigned to the $(\underline{70}, 1^-)$, $(\underline{56}, 2^+)$, and $(\underline{56}, 0^+)^*$ (radially excited) supermultiplets.⁶ By supplementing our fits with higher-energy data from Ayed and Bareyre¹² we further identify most of the $(\underline{70}, 3^-)$ states. In addition, we have fits with S_{31} resonances at 1635 and 2060 MeV, P_{33} resonances at 1690 and 2100 MeV, and D_{33} resonances at 1690 and 2070 MeV. These partial waves could have additional unresolved structure above 1850 MeV.

The $I = \frac{1}{2}$ partial waves are more erratic, because the π^-p elastic data are less precise than the π^+p data and because there is not much charge-exchange data. The D_{13} partial wave has a second resonance at 1655 MeV, a higher resonance near 2070 MeV, and structure at 1900 MeV which is consistent with (but does not require) a resonance of elasticity = 0.06. We find an $S_{11}(1630)$ and a $P_{11}(1810)$, but above about 1800 MeV these two partial waves are somewhat erratic (and highly correlated statistically) so there could be additional resonances with elasticities up to about

0.2. In general, odd-parity resonances with $J \leq \frac{3}{2}$, which could be assigned to a $(\underline{56}, 1^-)$ or to a second $(\underline{70}, 1^-)$ supermultiplet, are not required by our analysis, but they are also not excluded.

Since we believe the existence of the $D_{35}(1925)$ to be quite certain, we have further investigated its phenomenological implications. A D_{35} resonance can be accommodated by either a $(\underline{70}, 3^-)$ or a $(\underline{56}, 1^-)$ supermultiplet. We consider a $(\underline{70}, 3^-)$ assignment for the $D_{35}(1925)$ unlikely, because the mass of the observed state seems to be too low. Assuming a unit Regge slope, a recurrence of the $S_{31}(1635)$ member of the $(\underline{70}, 1^-)$ would be expected near 2200 MeV; such a mass would be consistent with the masses of other states assigned to the $(\underline{70}, 3^-)$ provided the symmetry-breaking pattern is similar to that in the $(\underline{70}, 1^-)$. In fact, our D_{35} partial wave amplitudes, when combined with higher-energy values from Ayed and Bareyre¹² are consistent with the existence of a second D_{35} resonance in the 2200- to 2400-MeV region. Therefore we consider the $D_{35}(1925)$ to be a member of a new supermultiplet, a $(\underline{56}, 1^-)$, which would also contain S_{11} , D_{13} , S_{31} , and D_{33} resonances. Our present analysis is consistent with the existence of these four resonances, but does not require them.

The familiar three-quark harmonic-oscillator model^{1,2} does not predict a $(\underline{56}, 1^-)$ supermultiplet in the 1900-MeV region. Dual string models,⁴ however, suggest the existence of additional daughter states degenerate with those on leading trajectories. To pursue this idea in a phenomenological model, we consider baryons to be made up of four massless partons: three valence quarks and a neutral, colorless, scalar "monad" which represents the energy and momentum carried by gluon fields or nonvalence quarks. The leading term in the potential energy is proportional to the minimum possible length of "colored strings" required to join the partons; at least one string is attached to each quark, at least two strings are attached to the monad, and a vertex with three intersecting strings is allowed. This potential energy favors states in which the partons lie along a line. If there is a quark at each end of the line, a single string can join all the partons, otherwise a doubled string is required. For configurations in which the partons form two clusters, an asymptotic calculation gives

$$M^2 = 8KT \left[L + \frac{1}{2} + \sqrt{2}(N + \frac{1}{2}) \right] + O(1/L),$$

where L is the orbital angular momentum, N is the number of radial nodes, T is the tension of

the strings, and K is their number. An exact calculation shows that the asymptotic expression is accurate to a few percent for all L and N . For $K=1$ we have the usual quark-diquark states,³ $(\underline{56}, L_{\text{even}}^+)_1$ or $(\underline{70}, L_{\text{odd}}^-)_1$, while $K=2$ leads to $(\underline{56}, L^\pm)_2$ supermultiplets. The new supermultiplet $(\underline{56}, 1^-)_2$ is nearly degenerate with the normal $(\underline{56}, 2^+)_1$. Note also that the radially excited $(\underline{56}, 0^+)_1^*$ has a lower energy than the $(\underline{56}, 2^+)_1$, which agrees with the observed masses of the P_{11} and P_{33} resonances.

We acknowledge valuable discussions with J. W. Alcock, Y. A. Chao, D. P. Hodgkinson, R. G. Lipes, and J. C. Sandusky, and also their aid in developing the computer programs which have been used in this analysis.

*Work supported by the U. S. Energy Research and Development Administration.

¹O. W. Greenberg, Phys. Rev. Lett. **13**, 598 (1964); O. W. Greenberg and M. Resnikoff, Phys. Rev. **163**, 1844 (1967).

²R. P. Feynman, M. Kislinger, and F. Ravndal, Phys. Rev. D **3**, 2706 (1971).

³A. N. Mitra and D. L. Katyal, Nucl. Phys. **B5**, 308 (1968); D. B. Lichtenberg, Phys. Rev. **178**, 2197 (1969).

⁴See, for example, S. Mandelstam, Phys. Rep. **13C**, 260 (1974); I. Bars and A. J. Hanson, Phys. Rev. D **13**, 1744 (1976).

⁵A. Chodos *et al.*, Phys. Rev. D **9**, 3471 (1974), and **10**, 2599 (1974); W. A. Bardeen *et al.*, Phys. Rev. D **11**, 1094 (1975).

⁶R. Horgan and R. H. Dalitz, Nucl. Phys. **B66**, 135 (1973).

⁷D. P. Hodgkinson *et al.*, Lawrence Berkeley Laboratory Report No. LBL-3048, 1974 (unpublished).

⁸R. E. Cutkosky and B. B. Deo, Phys. Rev. **174**, 1859 (1968).

⁹J. W. Alcock and W. N. Cottingham, Nucl. Phys. **B41**, 141 (1972), and private communication.

¹⁰R. E. Cutkosky *et al.*, Nucl. Phys. **B102**, 139 (1976).

¹¹J. R. Carter *et al.*, Nucl. Phys. **B58**, 378 (1973).

¹²R. Ayed and P. Bareyre, private communication.

¹³Y. A. Chao *et al.*, Phys. Lett. **57B**, 150 (1975).

¹⁴T. G. Trippe *et al.*, Rev. Mod. Phys. **48**, S1 (1976). See p. S147.

¹⁵Trippe *et al.*, Ref. 14. See pp. S183-S186.

Observation of Elastic Antineutrino-Proton Scattering*

D. Cline, A. Entenberg, W. Kozanecki, A. K. Mann, D. D. Reeder, C. Rubbia, J. Strait, L. Sulak, and H. H. Williams

Department of Physics, Harvard University, Cambridge, Massachusetts 02138, and Department of Physics, University of Pennsylvania, Philadelphia, Pennsylvania 19174, and Department of Physics, University of Wisconsin, Madison, Wisconsin 53706

(Received 18 June 1976)

We have observed 22 events of the process $\bar{\nu}p \rightarrow \bar{\nu}p$ with a background expectation of 8 events. The neutral-current-to-charged-current ratio $\sigma(\bar{\nu}p \rightarrow \bar{\nu}p)/\sigma(\bar{\nu}p \rightarrow \mu^+n)$ is measured to be 0.2 ± 0.1 for $0.3 < q^2 < 0.9$ (GeV/c)², where $-q^2$ is the square of the four-momentum transfer to the proton. When combined with our previous measurement of $\nu p \rightarrow \nu p$, this yields a ratio $\sigma(\bar{\nu}p \rightarrow \bar{\nu}p)/\sigma(\nu p \rightarrow \nu p) = 0.4 \pm 0.2$, where the error is statistical, suggesting that a purely vector, neutral, hadronic current is unlikely.

Because of their simplicity, two of the most interesting weak neutral current reactions are the elastic scattering by protons of neutrinos and antineutrinos. Both the cross section magnitudes and the shapes of $d\sigma/dq^2$ are experimentally accessible, providing a sensitive measure of the space-time transformation properties of the weak hadronic neutral current. Any difference between neutrino and antineutrino elastic scattering is a direct signature of parity nonconservation in the matrix element of the hadronic current. We have recently reported results on a measurement¹ of $\nu p \rightarrow \nu p$. This paper reports the first observation of elastic antineutrino-proton scattering. A pre-

vious search² for the reaction $\bar{\nu}p \rightarrow \bar{\nu}p$ was hampered by high neutron background and low statistics; whereupon only an upper limit was obtained.

The experiment was performed at the Brookhaven National Laboratory (BNL) in a "wide-band" horn-focused antineutrino beam. The target-detector, 33 tons of liquid scintillator with drift chambers interspersed, has previously been described.^{1,3,4} The antineutrino data reported here were taken shortly after our previous neutrino run.¹ The integrated ν and $\bar{\nu}$ fluxes and the running conditions were comparable for the two runs, thus minimizing any systematic effects.

An energy deposition greater than 3 MeV in any